Line Length and Fault Distance Considerations in Traveling-Wave Protection and Fault-Locating Applications

Bogdan Kasztenny and Venkat Mynam
Schweitzer Engineering Laboratories, Inc.

Line Length and Fault Distance Considerations in Traveling-Wave Protection and Fault-Locating Applications

Bogdan Kasztenny and Venkat Mynam
Schweitzer Engineering Laboratories, Inc.

Abstract—**This paper analyzes the impact of line length, fault location, and locations of external and internal discontinuities on traveling-wave (TW) protection and fault-locating functions. The paper explains the underlying principles and derives a method to calculate the minimum line length that yields an expected level of accuracy and dependability. The paper serves as a tutorial on propagation and timing of TWs and is of interest to those practitioners who evaluate, test, apply, and troubleshoot TW-based devices. The paper is directly applicable to devices that use a window-based method for detecting and time-stamping TWs; however, the conclusions and findings can be extrapolated for devices that use any signal-processing method for detecting TWs.**

I. INTRODUCTION

Following positive field experience with traveling-wave (TW) fault locators [1] [2], we have successfully introduced TW-based line protection [3] with field installations starting in early 2017 [4]. To date, the following TW-based line protection, fault-locating, and line monitoring functions are available in protective relays and have been successfully deployed in the field [4] [5]:

- TW-based directional element, TW32.
- TW-based differential scheme, TW87.
- Single-ended TW-based fault locating, SETWFL.
- Double-ended TW-based fault locating, DETWFL.
- TW-based line monitoring, LM.

Additionally, the ultra-high-speed line protection includes the following incremental quantity-based elements:

- Incremental-quantity directional element, TD32.
- Incremental-quantity distance element, TD21.

In a typical application, the TD21 element is configured to trip directly without a protection channel, the TW32 and TD32 elements are used in a directional comparison pilot scheme, and the TW87 scheme is used when a direct fiber channel is available. A typical application uses phasor-based protection elements and schemes for dependability in cases where the time-domain protection restrains when the TW signals are too small or for other reasons [3]. Early microprocessor-based TW line protective relays required a standalone backup relay. Newer relays include phasor-based protection elements.

The double-ended TW-based fault-locating method (referred to in this paper as the double-ended method) can be applied over a multiplexed channel (IEEE C37.94 encoding) for data exchange and with IRIG-B-connected satellite clocks for time synchronization, or it can use a direct fiber channel for both data exchange and time synchronization. In both applications, the double-ended method does not require a dedicated channel but shares the channel with protection schemes. This avoids additional cost and complexity. The double-ended method allows a TW-based line monitoring function [6] for continuous line monitoring to detect, locate, and tabulate incipient or recurring line faults and fault precursors.

The single-ended TW-based fault-locating method (referred to in this paper as the single-ended method) works with data from the local line terminal and avoids the need for a digital channel and time synchronization.

Our field experience with time-domain protection is excellent. Relays [4] and [5] have been installed to protect well over a hundred lines, have restrained for thousands of external events, and have operated numerous times for internal faults. These line protective relays have an excellent security record and a good dependability record. The observed trip times are on the order of 2–8 ms for the TD21 element, 1–2 ms for the TW87 scheme, and 1–2 ms plus the channel time for the permissive overreaching transfer trip scheme. The fault-locating accuracy is on the order of one tower span as demonstrated in the field since 2013 [2] and since 2016 [4].

Measuring differences in TW arrival times and comparing polarities of TWs are at the heart of any TW-based protection or fault-locating method. Indeed, a TW-based method can be defined as one that responds to differences in TW arrival times or relative polarities of TWs. TW arrival times and polarities are robust signal features. When a TW is properly detected in signals acquired at high sampling rates, the arrival time and polarity of that TW are measured very accurately. The polarity and arrival time are principally independent from the signal magnitude, fault resistance, and many properties of the power system. Therefore, interfering signals cannot easily alter and influence the TW polarity and arrival time.

Reliable detection of TWs in a stream of signal samples depends, however, on sufficient time separation between successive TWs. If two or more TWs arrive in quick succession, a TW-based relay or a fault locator may have difficulties separating these TWs from one another. A blunt instrument of faster sampling would not necessarily solve the problem because the frequency response of instrument transformers and secondary cables would become limiting factors [1]. A relay or a fault locator can detect and time-stamp two TWs only if the

second TW arrives after a certain delay. To arrive separated by a certain minimum time, the two TWs must travel two distances that differ by a certain minimum distance.

The following situations may lead to a train of TWs that arrive in quick succession:

- Very short lines where the end-to-end TW travel time is very short.
- Faults very close to either line terminal or close to any discontinuity on the line (such as a line tap).
- Applications with very short lines connected to the same bus as the protected line.

The impact of TWs arriving in quick succession is different for different protection and fault-locating functions and TW-detection methods. Moreover, the impact of insufficient TW separation is not necessarily a total loss of function but is rather a gradual loss of protection dependability and fault-locating accuracy.

This paper discusses the line length challenge and other related issues as they apply to TW-based protection, fault locating, and line monitoring functions. The conclusions are directly applicable to functions implemented in [4] and [5] but may be extrapolated to other implementations. The paper is organized as follows:

- Section II explains TW-detection and time-stamping methods and focuses on the differentiator-smoother filter used in [4] and [5] and used in a slightly different form in [2].
- Section III explains the proximity effect when a fault is located too close to a discontinuity on the protected line, including line terminals and line taps, or too close to a discontinuity external to the protected line.
- Section IV explains the issue of TWs aliasing, where multiple TWs arrive at the same time because they traveled the same distance after being reflected several times.
- Section V discusses the case of a short line where TW reflections from the opposite terminal arrive so early that they blend with the TW from the fault. It also discusses long cable lines and the issue of TW attenuation and dispersion.
- Section VI introduces the concept of TW-based fault-locating dependability as it applies to line length and location of the fault.
- Section VII briefly discusses fault analysis and offline fault-locating calculations as they relate to line length, fault location, TW aliasing, and proximity effects.
- Section VIII discusses in detail the accuracy of TW-based fault-locating methods and the dependability of TW-based protection elements and schemes [4] [5].

We recommend that readers review the principles of operation of the discussed protection and fault-locating functions by reading [1], [3], [6], and [7].

II.   TW DETECTION AND TIME-STAMPING

TWs are surges of electricity launched by a sudden change in voltage, such as a line fault, that propagate at about 98 percent of the speed of light in free space on overhead lines and at about 45 to 85 percent of the speed of light in free space on cable lines. Ethylene propylene rubber cable insulation results in a propagation velocity at the lower end of the range, oil filled paper insulation results in a propagation velocity at the upper end of the range, and cross-linked polyethylene insulation yields a propagation velocity in the middle of the range. For simplicity, this paper uses 70 percent propagation velocity when discussing cable lines. From the measurement and signal processing perspectives, a TW is a step change in current or voltage with transition times on the order of a few microseconds. Fig. 1 shows an ideal TW in the signal x (current or voltage). The TW in Fig. 1 arrives at time t_0, has a positive polarity (the signal stepped up), and an instantaneous magnitude of A_0. The pre-step and post-step signal values appear flat because the figure shows a very short span of time (microseconds), not allowing the curvature of the fundamental frequency alternating current (ac) signal component to be visible.
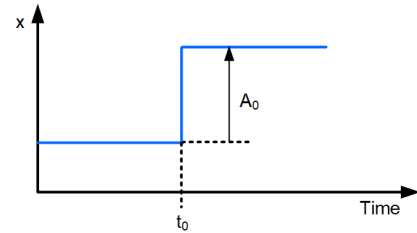

Fig. 1.   TW in the input signal x.

Protection and fault-locating functions in [4] and [5] use a differentiator-smoother (DS) filter [1] to detect TWs. A DS filter is a finite-impulse response filter (FIR) with a data window, as shown in Fig. 2. The DS filter is a least-square best-fit estimator for a step signal pattern. This is analogous to the Fourier filter being a least-square best-fit estimator for a sine wave signal pattern. The DS filter detects step changes in the input signal, the same way the Fourier filter detects sine waves in the input signal. Based on the concept of a data window, the DS-based method for detecting TWs can be referred to as a window-based method. Other methods are possible [1] and have been both applied in the field and proposed in literature. This paper focuses on window-based TW-detection methods.

We denote the half-length of the DS filter window as TWDSW (TW differentiator-smoother window). The gain coefficient for the filter is 1/TWDSW to ensure that the DS filter output corresponds to the instantaneous TW magnitude, at least when the TW front is sharp. As with any FIR filter, the DS filter has a group delay equal to half its data window length, i.e., the group delay is TWDSW.
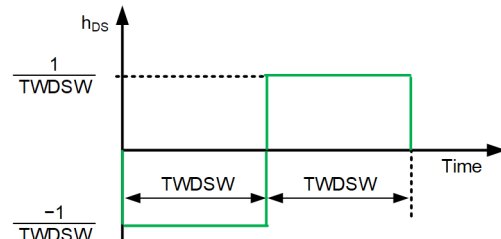

Fig. 2.   DS filter data window.

In a practical TW-based device, the TWDSW parameter is on the order of several microseconds. Long DS filter windows allow better noise suppression. Short DS filter windows allow detecting TWs that arrive separated by less time. Protection and fault-locating functions in [4] and [5] use a common DS filter for fault locating and TW-based protection. Therefore, their DS filter data windows are relatively long (TWDSW = 10 μs) striking a good balance between protection, security, and time-stamping resolution. Device [2] provides TW-based fault locating only and it uses a shorter DS filter data window, on the order of 3 μs.

Fig. 3 shows the response of the DS filter to an ideal TW and a dispersed TW (dispersion refers to the wavefront losing its steepness as the TW travels over a long distance). The filter output has a triangular shape when subjected to an ideal TW. The peak of the output waveform represents the instantaneous TW magnitude (including the TW polarity), and the time of the peak represents the TW arrival time (with a constant group delay of TWDSW).

TWs encounter dispersion when they travel on lossy lines. Dispersion causes the TW front to lean rather than be an ideal step (compare Fig. 3(b) and Fig. 3(a)). The DS filter responds with a parabola-shaped output to dispersed TWs. TW time-stamping algorithms in [2], [4], and [5] fit a parabola to the samples near the DS filter output peak and calculate the time of the peak (TW arrival time) as the time when the best-fit parabola is at its extremum [1]. This approach results in additional noise rejection and allows time-stamping resolution that is approximately five times better than the device sampling rate; for example, one can obtain an effective 0.2 μs time resolution when sampling every 1 μs.
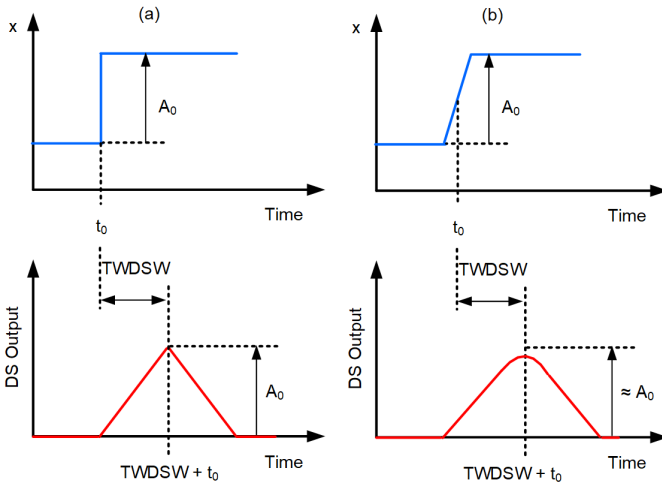

Fig. 3. DS filter response to (a) an ideal TW and (b) a dispersed TW.

Fig. 3(a) illustrates that the DS filter settles completely in a time equal to $2 \cdot$ TWDSW. When the TW is dispersed, the DS filter settling time is slightly longer ($2 \cdot$ TWDSW plus the time of the TW transition from the pre-step to post-step levels, see Fig. 3(b)). When the filter settles, the step change in the input signal is entirely removed from the filter data window – the filter completely processed and "forgot" the previous TW and is ready to process the next TW.

Fig. 4 shows a case of two ideal TWs that arrive in quick succession. The figure uses a TWDSW = 10 μs for detecting TWs. Fig. 4(a) shows the first TW that arrives at 0 μs (the step change from 0.5 to 1.5 in the signal level) and the second TW that arrives at 30 μs (the step change from 1.5 to 2 in the signal level). The two peaks in the DS filter output signal represent the TW magnitudes (1 and 0.5 respectively) and arrival times (DS filter output peaks are at 10 μs and 40 μs, respectively, and are consistently shifted by the 10 μs group delay of the DS filter with respect to the true arrival times of 0 μs and 30 μs).
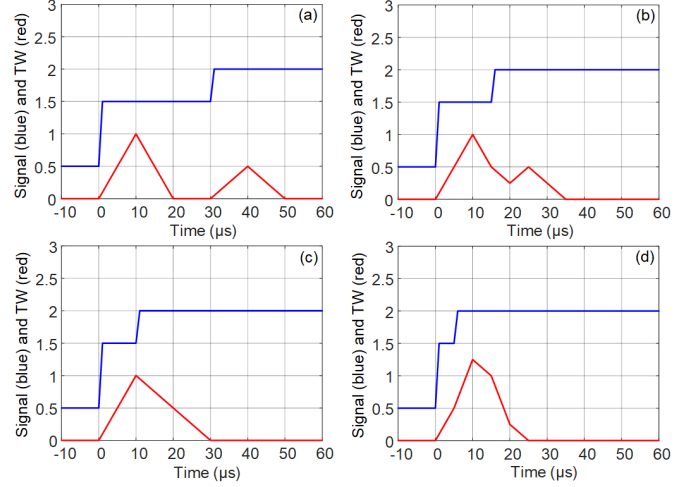

Fig. 4. DS filter response to two TWs that arrive in quick succession (the second TW is smaller than the first TW).

Fig. 4(a) shows a case where the second TW arrives after a time longer than $2 \cdot$ TWDSW. In this case, the DS filter fully separates (detects and correctly time-stamps) both TWs.

Fig. 4(b) shows a case where the second smaller TW arrives when the DS filter output was halfway down (TWs are separated by $0.75 \cdot 2 \cdot$ TWDSW). In this case, the second TW starts exciting the filter before the filter has settled after the previous TW. We can still see two separate peaks in the DS filter output. The times of the two peaks correspond to the true arrival times of the TWs. If the TW-detection algorithm (peak-finding algorithm) is designed to select both peaks in the DS filter output, the time stamps of the two TWs are correct.

Fig. 4(c) shows a case where the second smaller TW arrives when the DS filter output was at its peak (TWs are separated by $0.5 \cdot 2 \cdot$ TWDSW). In this case, the two TWs blend in the DS filter window. The DS filter output shows only one peak, and the time of the peak corresponds to the first TW.

Fig. 4(d) shows a case where the second smaller TW arrives when the DS filter output was halfway up (TWs are separated by $0.25 \cdot 2 \cdot$ TWDSW). The two TWs blend and the time stamp corresponds to the first TW.

The second TW in Fig. 4 has a magnitude less than the first TW. Consider, however, an opposite case when the second TW has a magnitude greater than the first TW (see Fig. 5). Fig. 5 teaches us that when the two TWs blend and the second TW is larger, the time stamp of the blended TW corresponds to the second TW, not the first TW.
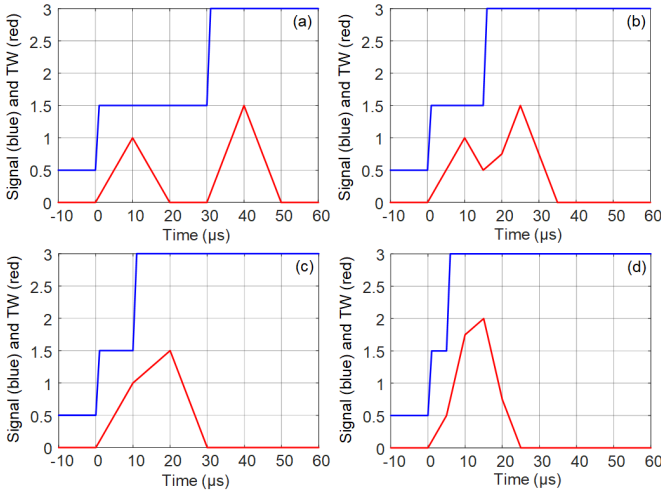
Fig. 5. DS filter response to two TWs that arrive in quick succession (the second TW is larger than the first TW).

Fig. 6 shows two more ways in which two successive TWs can blend. If two TWs have similar magnitudes and arrive in quick succession, the DS filter output can have an ill-defined peak (flat top), see Fig. 6 (a). The flat top challenges the peak-finding and parabola-fitting algorithms, and it may result in poor accuracy of the time stamp. In Fig. 6(a), the time of the DS filter output peak is between 10 and 15 µs, pointing to a TW arrival time of between 0 and 5 µs (the first TW arrived at 0 µs and the second TW arrived at 5 µs). Fig. 6(b) shows a case when the second TW has an opposite polarity relative to the first TW. In this case, the first TW is time-stamped correctly, but the second negative DS filter output peak occurs at 20 µs, suggesting that the second TW arrived at 10 µs. In reality, the second TW arrived at 5 µs; the time-stamping error for the second TW is therefore 5 µs. Two TWs that are of opposite polarities and arrive in quick succession create an impulse, and the DS filter output becomes an impulse response of the DS filter, i.e., it resembles the DS filter data window (compare Fig. 2 and Fig. 6(b).
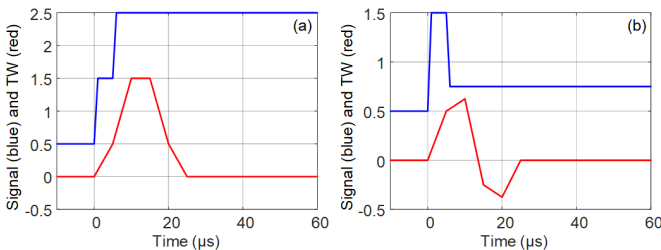

Fig. 6. DS filter response to two TWs that arrive in quick succession: (a) ill-defined peak and (b) second TW time stamp is inaccurate.

Fig. 4, Fig. 5, and Fig. 6 teach us that a TW that follows the first TW by less than $2 \cdot$ TWDSW may either skew the TW arrival time or prevent the TW-detection algorithm from finding either or both TWs in the input signal.

Expect the following when TWs follow in quick succession:

- Two TWs that arrive at least $2 \cdot$ TWDSW apart are correctly detected and time-stamped.
- Two TWs that arrive separated by more than $1.5 \cdot$ TWDSW but less than $2 \cdot$ TWDSW may be correctly detected, or they may blend depending on the ratio of the TW magnitudes.
- Two TWs that arrive separated by less than about $1.5 \cdot$ TWDSW will always blend. The TW-detection algorithm will see them as a single TW. The time stamp will be biased toward the TW with the greater magnitude.
- If two TWs have similar magnitudes and they arrive in quick succession and blend, the DS filter output may have an ill-defined peak (flat top), challenging the accuracy of the time-stamping algorithm.
- TW dispersion extends the DS filter window settling time and makes detecting TWs that arrive in quick succession slightly more difficult.

For example, a device with a TWDSW = 10 µs, such as [4] and [5], correctly detects TWs that arrive separated by at least 20 µs, the device blends TWs that arrive separated by less than about 15 µs, and it may – depending on the TW function – work with lower dependability and accuracy for TWs that arrive separated by more than about 15 µs and less than 20 µs.

Traveling for 20 µs on an overhead line, a TW traverses about 6 km (3.7 mi). Traveling for 20 µs on a cable line, a TW traverses 4 km (2.5 mi). Therefore, a device that uses a 10 µs DS filter can reliably detect and time-stamp two TWs if they travel distances that differ by about 6 km (3.7 mi) on overhead lines or 4 km (2.5 mi) on cable lines. In the next sections, we discuss scenarios where the above requirement of the minimum distance difference is not met.

III. PROXIMITY EFFECT

By *proximity effect*, we mean a situation where two or more TW discontinuities are located very close to one another. This includes the fault (first discontinuity) located close to a line terminal, line tap, or an overhead-to-cable transition point. It also includes cases when two discontinuities are located close to one another irrespective of the fault location, such as a line tap and a line terminal, two line taps, or a line terminal and a terminal of a very short line connected to the terminal.

A. First Approximation of the TW Pattern

Consider a close-in fault on a two-terminal line, as shown in the Bewley diagram in Fig. 7. The fault is located at the distance M (mi or km) from the local terminal (L). The fault launches two incident TWs that travel away from the fault and toward the two line terminals. The first TW that arrives at the local terminal (TW_{L1}) partially reflects from the terminal and travels back to the fault. Part of that TW reflects from the fault and travels back to the local terminal, arriving as the second local TW (TW_{L2}). The process repeats several times until the TWs subside and dissipate. We can also expect that the TWs partially transmit through the fault and arrive at the remote terminal as a similar series of TWs in quick succession (TW_{R1}, TW_{R2}, TW_{R3}, and so on). TWs that arrive at the remote terminal reflect and travel back to the fault. When they reach the fault and the nearby local terminal, they reflect and travel back to the remote terminal. TWs at both the local and remote terminals come in bursts of several TWs in quick succession.
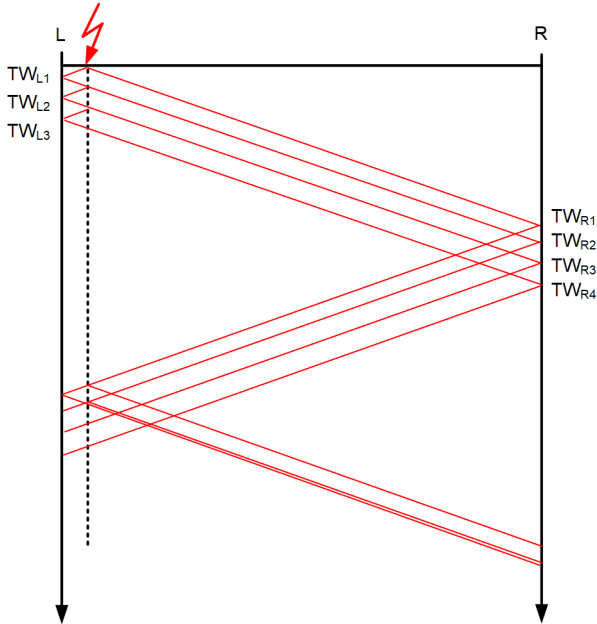
Fig. 7. Fault close to a line terminal results in a series of TWs in quick succession (first approximation).

If the distance M is sufficiently long, the DS filter can detect consecutive TWs (see Fig. 4(a) and Fig. 4(b)). If the distance is too short, the TWs will blend (see Fig. 4(c) and Fig. 4(d)), preventing detection of individual TWs and potentially skewing the time stamp of the first TW. According to this first approximation, the problem is not limited to the local terminal. Both the local and remote terminals receive a train of TWs in quick succession, irrespective of if the fault is very close to the local or remote terminal.

Fig. 8 shows a similar application challenge of a fault being close to a line tap. A line tap is a reflection point for TWs. TWs travel back and forth between the fault (F) and the tap (T) causing a train of TWs to arrive at both line terminals.
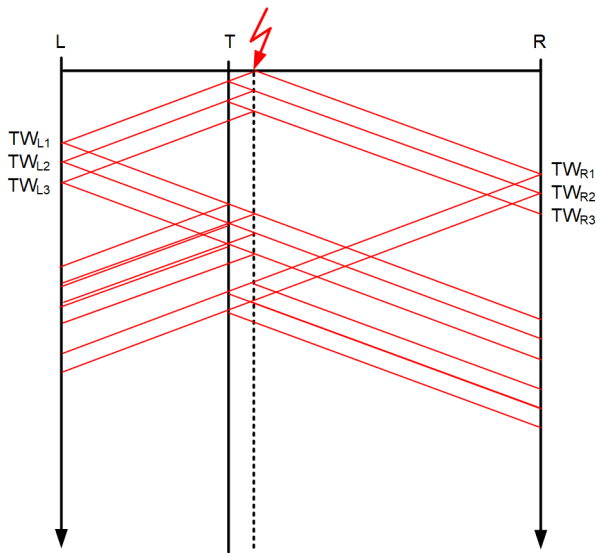

Fig. 8. Fault close to a line tap results in a series of TWs in quick succession (first approximation).

Fig. 7 and Fig. 8 show that two discontinuities that are close to each other generate a series of TWs in quick succession. As this series propagates away and reflects off other discontinuities, the TWs multiply and overlap.

The time difference between two consecutive TWs in Fig. 7 and Fig. 8 is proportional to the round-trip TW travel time between the fault (F) and the terminal (L in Fig. 7) or between the fault and the tap (T in Fig. 8).

According to this first approximation, the proximity phenomenon does not impact devices that use a TWDSW = 10 μs when the distance between the fault and the discontinuity is longer than 3 km (1.8 mi) for overhead lines or 2 km (1.2 mi) for cable lines. When the distance is shorter, TWs can overlap, and the TW-based functions may be impacted. The first approximation, however, is a simplification that leads to overly conservative observations.

B. Actual TW Pattern

A fault launches TWs only in the faulted phase(s). For example, a Phase-A-to-ground fault only launches a TW in Phase A. As the TW travels along a three-phase line, some energy couples from the faulted phase to the healthy phases (Phases B and C for a Phase-A-to-ground fault). However, for this coupling to be effective, a TW must travel some distance [1], such as about 20 to 30 km (12 to 18 mi). If the fault is very close to a line terminal, no TWs will develop in the healthy phases. Therefore, the TW arrives and reflects from the line terminal only in the faulted phase. This reflected TW arrives back at the fault, but because it traveled only a short distance, it too arrives only in the faulted phase. When this TW encounters the fault, it reflects almost completely and travels back to the terminal. Only a very small portion continues to the remote terminal on the faulted phase because the fault has a low characteristic (surge) impedance. TWs in the healthy phases would have passed through the fault location and continued to the remote terminal, but the magnitude of these TWs is close to zero (the healthy phases have not coupled any energy from the faulted phase because of the short distance traveled). Therefore, no, or very small, TWs transmit through the fault and continue toward the remote terminal.

Phase-to-phase faults do not create large TWs in the healthy phase. The coupling from the two faulted phases on the third healthy phase cancel. Conductor placement asymmetry is the only reason for any TW energy to couple to the healthy phase during phase-to-phase faults.

Three-phase faults do not allow TWs to propagate through the fault because all three conductors include the fault (the fault resistance is considerably less than the line characteristic impedance, and therefore the fault has a very low characteristic impedance in all three phases).

Considering all fault types, we can make the following observations for faults close to a terminal:

- The local terminal measures TWs only in the faulted phase(s).
- Multiple TWs arrive at the local terminal in quick succession, with magnitudes less than the first TW.
- The remote terminal measures only the initial TW. This TW typically has the expected three-phase

pattern (the faulted and healthy phases) because the TW traveled a long distance.

- TW reflections from the local terminal do not propagate through the fault and do not arrive at the remote terminal.

Based on the above observations, Fig. 9 and Fig. 10 show more realistic Bewley diagrams for the cases from Fig. 7 and Fig. 8, respectively. These diagrams account for the effect of TW propagation through the fault (a TW will not propagate through the fault if it has not traveled a long enough distance prior to arriving back at the fault).

Fig. 9 shows a series of TWs between the fault and the local terminal. These TWs, however, do not propagate through the fault. The remote terminal receives a single initial TW (TW_{R1}). This TW, when reflected from the terminal, travels back and reflects from both the fault and the local terminal. As a result, the first reflection from the fault (TW_{R2}) is followed by a reflection from the local bus (TW_{R3}). The operating conditions for the single-ended method at the remote terminal are much more favorable compared with the local terminal.
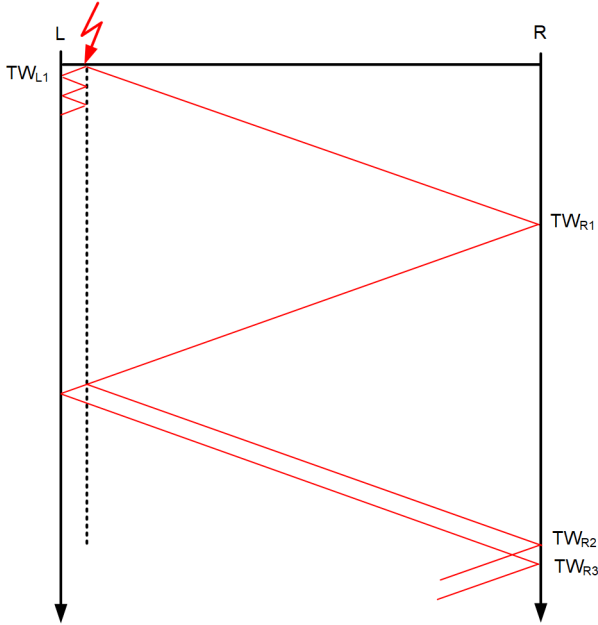

Fig. 9. Fault close to a line terminal (practical pattern).

Fig. 10 shows a series of TWs between the fault and the tap. These TWs, however, do not propagate through the fault. The remote terminal receives a single initial TW (TW_{R1}). This TW, when reflected from the terminal, travels back and reflects from both the fault and the tap. As a result, the first reflection from the fault (TW_{R2}) is followed by a reflection from the tap (TW_{R3}). The operating conditions for the single-ended method at the terminal that does not have a tap between the terminal and the fault (remote terminal in Fig. 10) are more favorable compared with the terminal that has a tap between the terminal and the fault (local terminal in Fig. 10).

The cases in Fig. 9 and Fig. 10 are even more favorable than the Bewley diagrams imply because TWs attenuate each time they reflect or transmit through a discontinuity. For example, TW_{R2} has a magnitude greater than TW_{R3} in both figures.
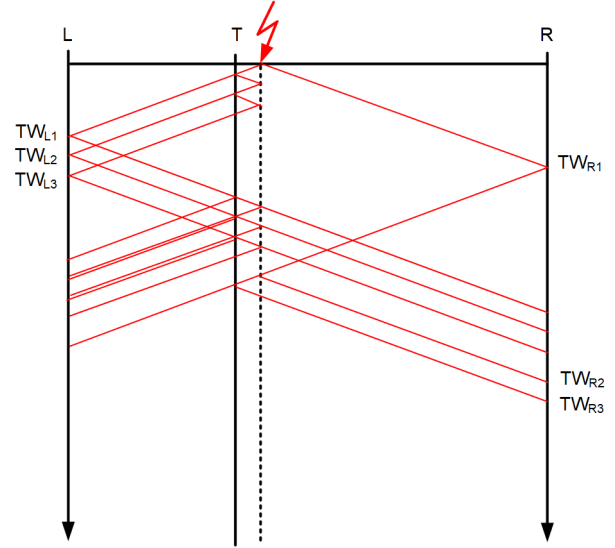

Fig. 10. Fault close to a line tap (practical pattern).

C. Field Case Example

Fig. 11 shows the local and remote currents and current TWs for a Phase-C-to-ground fault on a 69 kV line [8]. The line is only 8.49 mi long (end-to-end TW propagation time of 46.51 μs), and the line crew found the fault at 2.01 mi from the local terminal.

Fig. 11 shows the initial TW at the local terminal (−173 A primary) and the first reflection from the fault (−70 A primary), separated by 22.318 μs. Two more reflections from the fault are clearly visible in the local Phase C current. The local current TWs are near zero in the healthy phases (A and B) because no energy coupled to the healthy phases during the 2 mi travel from the fault to the local terminal. The remote current TWs in the healthy phases are near zero as well because the travel distance to the remote terminal is only 6.5 mi. The remote current TWs do not show any quick reflections resulting from TWs oscillating between the fault and the local terminal (the local current shows four clear reflections). The first TW at the remote terminal is about −186 A primary. The next major TW is the reflection from the fault after the round-trip time from the remote terminal to the fault (−98 A primary). The two TWs at the remote terminal are separated by 72.434 μs. The first TWs at the local and remote terminals are separated by 24.528 μs. The field case example in Fig. 11 confirms and illustrates the TW pattern in Fig. 9.

We calculate the TW-based fault location relative to the local terminal as follows.

Double-ended method:

$$M = \frac{8.49 \text{ mi}}{2}\left(1 - \frac{24.528 \text{ μs}}{46.51 \text{ μs}}\right) = 2.006 \text{ mi} \tag{1a}$$

Single-ended method at the local terminal:

$$M = \frac{8.49 \text{ mi}}{2} \cdot \frac{22.318 \text{ μs}}{46.51 \text{ μs}} = 2.037 \text{ mi} \tag{1b}$$

Single-ended method at the remote terminal (the calculation shows the distance from the local terminal):

$$M = 8.49 \text{ mi} - \frac{8.49 \text{ mi}}{2} \cdot \frac{72.434 \text{ μs}}{46.51 \text{ μs}} = 1.879 \text{ mi} \tag{1c}$$

The 1.879 mi value differs by only 0.12 mi with respect to the true value of 2.01 mi.
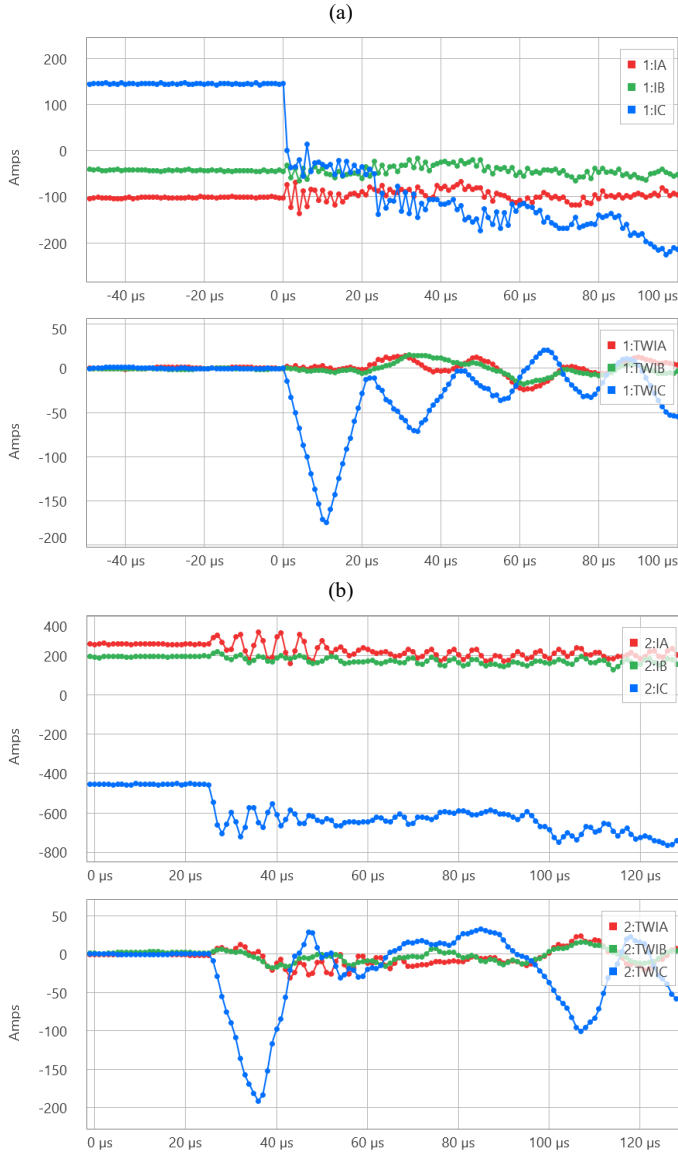

Fig. 11.   Local (a) and remote (b) currents and current TWs for a Phase-C-to-ground fault on an 8.49 mi line.

Fig. 11 and calculations (1) illustrate that TWs that have not traveled for at least about 12 mi do not propagate through a fault (the Bewley diagram in Fig. 9 is more accurate than the one in Fig. 7). The field case also illustrates the scenario of a close-in fault when the second TW arrives just after $2 \cdot TWDSW$ (arrival time difference of 22 µs compared with 20 µs); compare the local Phase C current TW in Fig. 11 to Fig. 4(a). Fig. 11 also illustrates the noise rejection capability of the DS filter: the Phase C current contains high-frequency noise, yet the DS filter output is relatively undistorted, allowing correct TW detection and time-stamping.

D.   Close-In Discontinuity External to the Protected Line

Fig. 12 shows a Bewley diagram for a line fault in a system with a discontinuity (Bus B) behind the local terminal. A portion of the first TW at the local terminal propagates toward the discontinuity and oscillates between Buses B and L. The

reflections from Bus B partially propagate through Bus L and travel to the fault and the remote terminal. As a result, the reflection from the fault measured at the local terminal has a form of several TWs in quick succession. Also, when the reflection from the local terminal arrives at the remote terminal, it has a form of several TWs in quick succession. The degree of impact of the discontinuity (Bus B) depends on the termination effect at Bus L. If the termination impedance is low (such as when many lines are connected to the bus), then only a small portion of the TW travels toward Bus B and an even smaller portion re-enters the protected line after reflection from the discontinuity (Bus B). Also, the termination impedance at Bus B plays a role. The worst-case scenario is when the termination impedance at Bus B is very low (such as when many lines are connected to the bus) or very high (such as termination with only a power transformer). Otherwise, only a fraction of the TW that reached Bus B travels back toward Bus L.
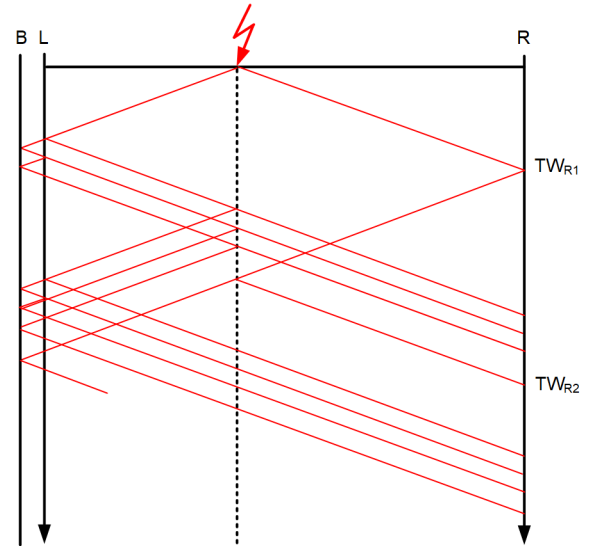

Fig. 12.   External discontinuity close to the line terminal results in a series of TWs in quick succession.

An external discontinuity that is close to a terminal blurs the TW reflected from the terminal and any other TW that originates from those reflections.

In general, the case of Fig. 12 does not affect the double-ended method and the single-ended method at the terminal that is away from the external discontinuity. The single-ended method at the local terminal may be affected by the challenge to detect the reflection from the fault (loss of function) and by the series of TWs reflected from Bus B, skewing the TW time stamp (degraded accuracy). However, the impact is real only if the termination impedance at Bus L is not low; otherwise, the reflections from Bus B are small and, therefore, inconsequential.

IV.   TRAVELING-WAVE ALIASING

We introduce the term *TW aliasing* to describe a scenario where two or more TWs arrive at the protection or fault-locating device at the same time after reflecting multiple times from various discontinuities in the network. The discontinuities are not necessarily close to each other. Only the total travel times are nearly identical.

Fig. 13 shows a case when the fault is located at a similar distance from the local terminal (L) as from an external bus (B). The TWs reflected from the fault and from Bus B arrive at a similar time (the blue oval shapes in the figure). The polarities of the two overlapping TWs may be the same or opposite depending on the termination impedance at Bus B. The two overlapping TWs can add together (see Fig. 6(a)) or partially cancel each other (see Fig. 6(b)), leading to an incorrect or skewed time-stamp value.
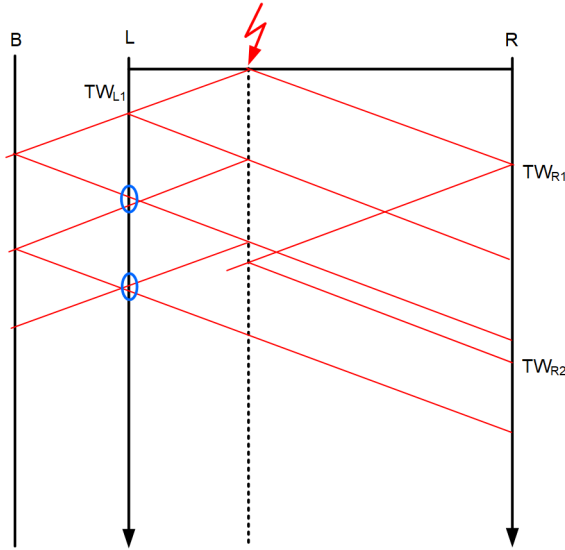

Fig. 13.   External discontinuity at a similar distance as the fault.

The operating conditions for the double-ended method are good because the first TWs at both line terminals (TW_{L1} and TW_{R1}) are not affected by the aliasing phenomenon. Also, it is unlikely that the aliasing would affect both terminals at the same time (the remote terminal receives the first reflection from the fault, TW_{R2}, without aliasing). The TW aliasing in Fig. 13 may affect the single-ended method at the terminal with the discontinuity behind it (L), but not the double-ended method, and it is not likely to affect the single-ended method at the terminal at the opposite end of the line (R).

Fig. 14 shows a case when the fault is located close to the line midpoint. The TWs reflected from the fault and from the remote terminal (R) arrive at the local terminal (L) at similar times. The polarity of the TW reflected from the remote terminal is typically opposite of the one reflected from the fault. The two TWs can partially cancel, or the reflection from the remote terminal can dominate the reflection from the fault. The two TWs can also blend, leading to an incorrect or skewed time-stamp value (see Fig. 6). When these TWs reflect from the terminal and travel back to the fault and the opposite terminal, they multiply, creating even more TWs that arrive again at the terminals. Again, the first TWs at both line terminals (TW_{L1} and TW_{R1}) are not affected, even though the subsequent TWs may be blurred (may overlap).
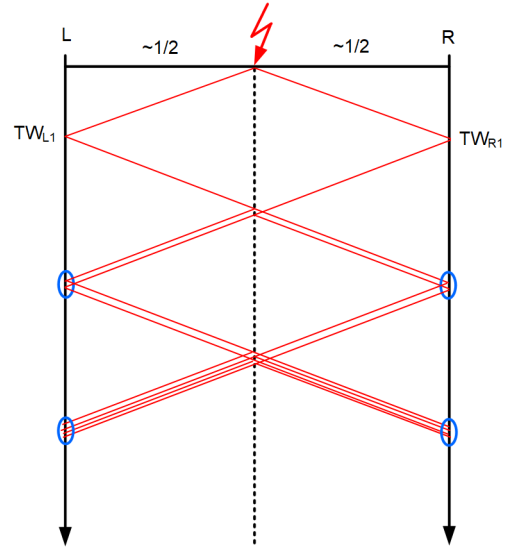

Fig. 14.   Fault near the line midpoint.

Fig. 15 shows a case when the fault is one-third of the line length from the local terminal and two-thirds from the remote terminal. The TW reflected from the remote terminal aliases with the second reflection from the fault (TW_{L3}).
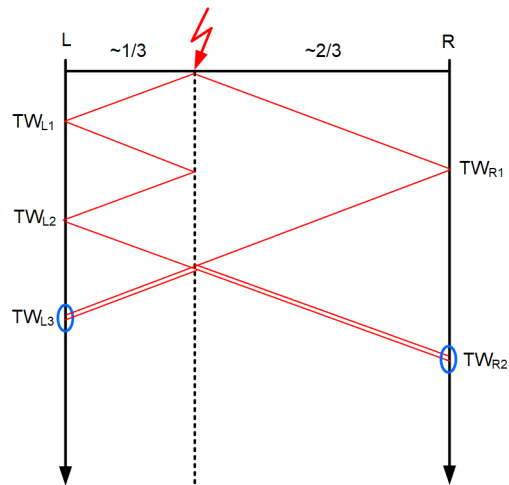

Fig. 15.   Fault near one-third of the line.

The cases in Fig. 13, Fig. 14, and Fig. 15 illustrate that the first TWs that arrive at both line terminals cannot alias and will always be measured correctly. Also, it is unlikely that TWs will alias at both line terminals (the fault at the line midpoint notwithstanding). As a result, aliasing does not impact the double-ended method. It may impact the single-ended method but typically at one terminal only.

Fig. 16 shows a case relevant for the TW87 scheme. A discontinuity (Bus B) is located at such a distance that it reflects a TW that arrives at the local terminal at the same time as the expected exit TW (a TW at Terminal L if the external fault (E) were beyond Terminal R). Normally, a reflection from the remote terminal arrives at the exit TW time. An external discontinuity may reflect a TW that arrives at the same time and it may impact the exit TW measurement in the TW87 scheme. This TW aliasing may impact the dependability (but not the security) of the TW87 scheme.
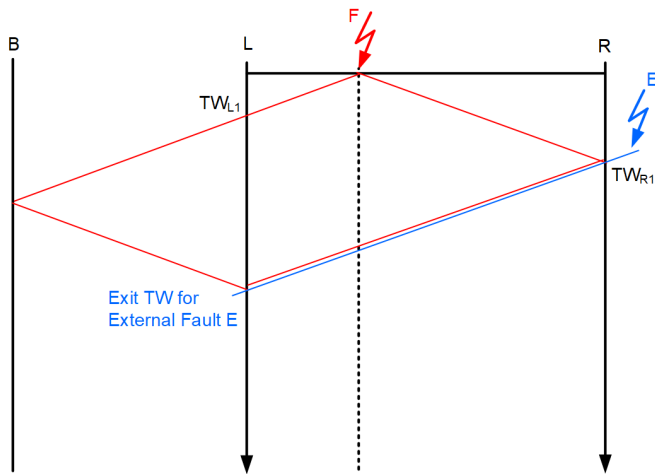
Fig. 16.   TW aliasing potentially impacting dependability of the TW87 scheme.

In this section, we showed examples of scenarios where TWs may overlap irrespective of the line length and irrespective of the distance to the fault or to a discontinuity. These scenarios can impact the accuracy of the single-ended method at one terminal of the line as well as the dependability of the TW87 scheme. The adverse effect is constrained to specific fault locations as they coincide with distances to discontinuities present in the system, irrespective of the line length. Termination impedances reduce the magnitudes of the aliasing TWs compared with the TWs that are expected and used by the TW-based functions.

V.   LINE LENGTH EXTREMES

A.   Short Lines

Fig. 17 shows a Bewley diagram for an internal fault on a very short line (overhead or cable). TWs reflected from the opposite line terminal arrive soon after the first TW arrives from the fault and may overlap with the TW from the fault given the DS filter window length.
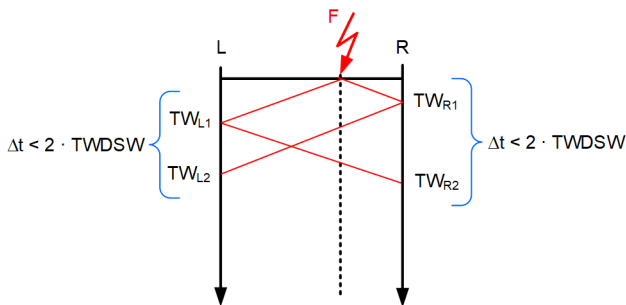

Fig. 17.   TWs overlap during an internal fault on a short line.

If the reflection from the opposite terminal (TW_{L2} for example) arrives quickly after the first TW from the fault (TW_{L1}), then the second TW (TW_{L2}) can either skew the time stamp of the first TW or it can make it difficult to detect the first TW (see Fig. 4). Note that the case of a short line is different than the close-in fault case in Fig. 9. In the case of a short line, both terminals experience TWs that arrive in quick succession. A close-in fault on a long line affects only the terminal that is closer to the fault.

Fig. 18 shows a Bewley diagram for an external fault behind the remote terminal of a short line. The first TW (TW_{R1}) is a reverse TW (arrives from behind the relay). TW_{R2} is a reflection from the local terminal and is a forward TW (arrives from the direction of the line). If these two TWs arrive in quick succession, then they may affect the security of the TW32 directional element. Voltage transformers will reproduce the polarity and timing of the first TW (TW_{R1}) but not necessarily the subsequent TWs (TW_{R2}) [1]. As a result, the presence of TW_{R2} could cause the TW32 element to declare a forward fault at Terminal R for the reverse fault in Fig. 18.
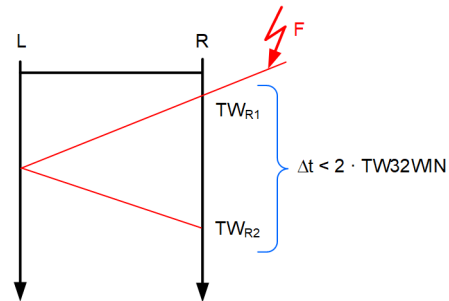

Fig. 18.   TWs for an external fault on a short line.

The TW32 element may use a data window, TW32WIN, such as 50 µs [4] [5]. You may be able to apply the TW32 element only when the line propagation time is longer than that window (see Section VIII for more information).

B.   Long Cable Lines

Cable lines are considerably more lossy than overhead lines and cause TWs to attenuate and disperse. Attenuation reduces the magnitude of the TW as it propagates along the line. Dispersion makes the front of the TW lean over as it propagates along the line.

The characteristic impedance of a cable line is approximately five times less than that of an overhead line (approximately 70 Ω compared to approximately 350 Ω). This means that faults on cable lines launch current TWs with magnitudes that are approximately five times greater than those on overhead lines (assuming the same fault voltage). This relative TW magnitude boost lessens the challenge of the attenuation.

Dispersion creates another challenge on long cable lines. Fig. 19 shows TWs with small dispersion (such as for an overhead line) and large dispersion (such as for a long cable line). To explain the dispersion challenge, the figure shows the DS filter output for the two TWs by using the TWDSW parameter of 3 µs and 10 µs.

When the DS filter window is sufficiently long compared with the TW "ramp-up" time (both 3 µs and 10 µs DS filter windows in Fig. 19(a)), the DS filter output has a well-defined peak and it correctly captures the TW magnitude (full sensitivity). When the DS filter window is short compared with the TW ramp-up time (3 µs DS filter window in Fig. 19(b)), the DS filter output does not have a well-defined peak (flat top), challenging the peak-detection and time-stamping algorithms, and it only captures a small portion of the TW magnitude (reduced sensitivity).
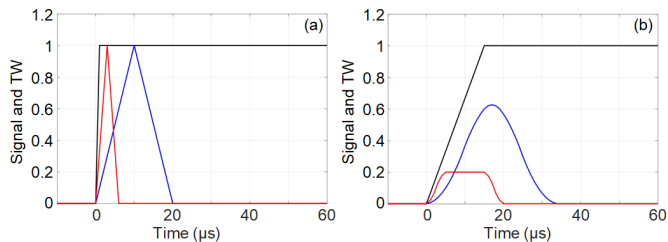
Fig. 19. TWs with small (a) and large (b) dispersion; DS filter with a 3 μs half-window (red) and 10 μs half-window (blue).

The DS filter window of 10 μs (default in implementations [4] and [5]) is sufficiently long to address attenuation in cable lines. The short DS filter window in [2] may be challenged in applications to long cables.

Very long cables may cause significant attenuation and dispersion and they may challenge the dependability of TW-based fault locators and the TW87 protection scheme.

VI. Fault-Locating Dependability

In this section, we use observations from Sections II through V and introduce a new concept of dependability contours for the double-ended and single-ended methods. A dependability contour is an area on a two-dimensional plane comprising the per-unit fault location (m) and the ratio of the DS filter window half-length (TWDSW) and the TW line propagation time (TWLPT).

Consider the following example. The TWDSW parameter of the TW-based fault-locating device is 10 μs and the length of an overhead line is 100 mi (TWLPT for the line is about 547 μs). Assume internal faults at 0.98 pu (98 mi) and 0.505 pu (50.5 mi). The first location is close to a terminal; the second location is close to the line midpoint. Dependability contours determine whether these faults are within the dependability limits of the double-ended and single-ended methods.

A. TW Arrival Time Analysis

Consider an internal fault at location m > 0.5 pu, as shown in the Bewley diagram in Fig. 20.
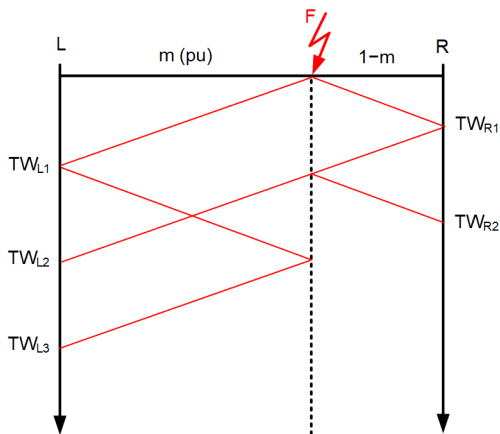

Fig. 20. Bewley diagram showing the five key TWs for an internal fault.

The diagram shows five TWs at the local and remote terminals that are key for TW-based fault locating. The TW arrival times for these five TWs are as follows:

$$t_{L1} = m \cdot TWLPT \tag{2a}$$

$$t_{L2} = (2 - m) \cdot TWLPT \tag{2b}$$

$$t_{L3} = 3 \cdot m \cdot TWLPT \tag{2c}$$

$$t_{R1} = (1 - m) \cdot TWLPT \tag{2d}$$

$$t_{R2} = 3 \cdot (1 - m) \cdot TWLPT \tag{2e}$$

We consider that two TWs can be reliably detected and time-stamped if they arrive at least $2 \cdot TWDSW$ apart. Therefore, TW_{L2} and TW_{L1} can be reliably detected if:

$$(2 - m) \cdot TWLPT - m \cdot TWLPT > 2 \cdot TWDSW \tag{3a}$$

Solving (3a) we obtain:

$$m < 1 - \frac{TWDSW}{TWLPT} \tag{3b}$$

Condition (3b) teaches us that that individually detecting TW_{L2} and TW_{L1} depends on the ratio of the TWDSW parameter and TWLPT. Therefore, we introduce an auxiliary variable δ as follows:

$$\delta = \frac{TWDSW}{TWLPT} \tag{4}$$

Inserting (4) into (3b), we can write that TW_{L2} and TW_{L1} are separated if:

$$m < 1 - \delta \tag{5}$$

Similarly, TW_{L3} and TW_{L1} are separated if:

$$3 \cdot m \cdot TWLPT - m \cdot TWLPT > 2 \cdot TWDSW \tag{6a}$$

Solving for m, we obtain:

$$m > \delta \tag{6b}$$

Similarly, TW_{L3} and TW_{L2} are separated if:

$$3 \cdot m \cdot TWLPT - (2 - m) \cdot TWLPT > 2 \cdot TWDSW \tag{7a}$$

Solving for m, we obtain:

$$m > \frac{1}{2}(1 + \delta) \tag{7b}$$

Finally, TW_{R2} and TW_{R1} are separated if:

$$3 \cdot (1 - m) \cdot TWLPT - (1 - m) \cdot TWLPT \\ > 2 \cdot TWDSW \tag{8a}$$

Solving for m, we obtain:

$$m < 1 - \delta \tag{8b}$$

The double-ended method works best if the first TWs at both terminals are separated from the consecutive TWs, i.e., when conditions (5), (6b), and (8b) are met. Because (5) and (8b) are identical, we can state that the double-ended method works well when:

$$m < 1 - \delta \ \textbf{and} \ m > \delta \tag{9}$$

The single-ended method at the local terminal works best if the first TW is separated from the first reflection from the fault (6b) and from the reflection from the remote terminal (5). Additionally, the reflection from the fault must be separated from the reflection from the remote terminal (7b). We can state

that the single-ended method at the local terminal works well when:

$$m < 1 - \delta \ \textbf{and} \ m > \delta \ \textbf{and} \ m > \frac{1}{2}(1 + \delta) \qquad (10a)$$

Condition (7b) is more restrictive than condition (6b); therefore, we can simplify (10a) and state that the single-ended method works well when:

$$m < 1 - \delta \ \textbf{and} \ m > \frac{1}{2}(1 + \delta) \qquad (10b)$$

Let us go back to our example of a TWDSW = 10 μs and a TWLPT = 547 μs (δ = 10/547 = 0.0183). Condition (9) tells us that the double-ended method is dependable for both fault locations, m = 0.98 pu and m = 0.505 pu. Condition (10b) tells us that the single-ended method is dependable for the fault location of 0.98 pu but not for the location of 0.505 pu.

B. Dependability Contours

We can represent condition (9) for the double-ended method and (10b) for the single-ended method as contours, see Fig. 21 and Fig. 22.

The shaded area in Fig. 21 is the dependability contour of the double-ended method. The vertical line in the figure represents a specific application (a TW-based fault-locating device with the TWDSW parameter and a power line with the propagation time of TWLPT). The intersection points of the vertical line with the shaded contour define the dependability limits for the double-ended method.

The upper shaded area in Fig. 22 is the dependability contour of the local single-ended method. The remote single-ended method has a contour that is a mirror reflection (the bottom shaded area). Assuming the application uses both the local and remote fault-locating results, the effective dependability contour includes both shaded areas. The potential overlap of the TW reflected from the fault and reflected from the opposite terminal (see Fig. 14) lowers the dependability for faults near the line midpoint.
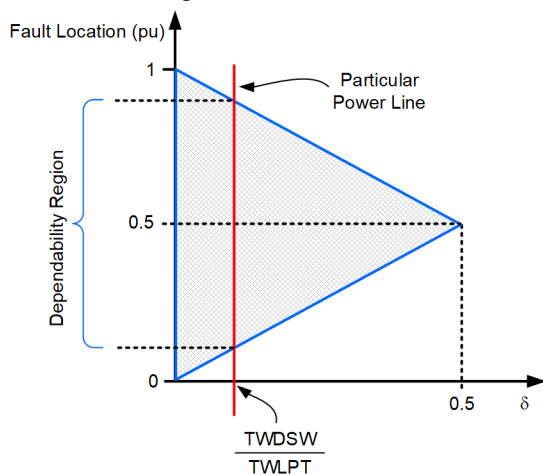

Fig. 21. Dependability contour for the double-ended method – graphical representation of (9).
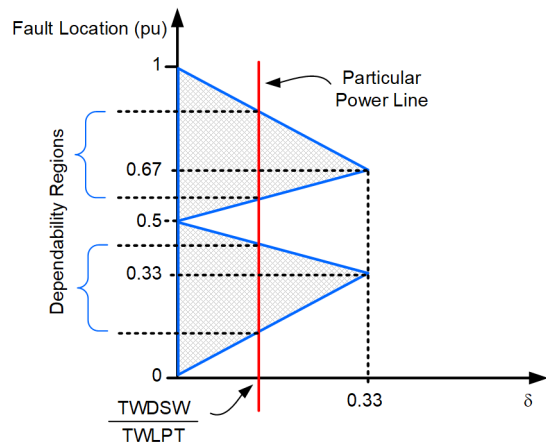

Fig. 22. Dependability contour for the single-ended method – graphical representation of (10b).

When the power line is long (small δ), the vertical line in Fig. 21 and Fig. 22 moves to the left and the dependability interval becomes larger. When the power line is short (large δ), the vertical line in Fig. 21 and Fig. 22 moves to the right and the dependability interval becomes smaller. Fig. 23 shows the percentage dependability of the double-ended and single-ended methods as a function of the parameter δ. Theoretically, the double-ended method does not work at all when δ > 0.5, i.e., when TWLPT < 2 · TWDSW. The single-ended method does not work at all when δ > 0.33, i.e., when TWLPT < 3 · TWDSW.
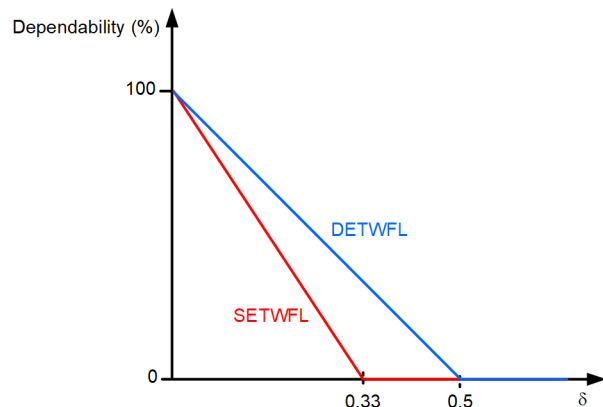

Fig. 23. Dependability of the double-ended and single-ended methods as a function of δ.

You can use Fig. 23 to decide on the minimum line length that justifies a TW-based fault-locating application. If 80 percent dependability is satisfactory, the corresponding δ is 0.100 for the double-ended method and 0.067 for the single-ended method. For a device with a TWDSW = 10 μs, the corresponding minimum line propagation times are therefore 100 μs and 150 μs, respectively. For an overhead line, these propagation times correspond to the length of 29.4 km (18.3 mi) and 44.1 km (27.4 mi) for the double-ended and single-ended methods, respectively. You can also use Fig. 23 to calculate the expected dependability for a given line length. For example, for a 100 mi line and a device with a TWDSW = 10 μs (δ = 0.0183), the double-ended method has a

theoretical dependability of 96 percent, and the single-ended method has a theoretical dependability of 94 percent.

Fig. 24 and Fig. 25 plot the dependability as a function of the TWLPT and line length, respectively, for a device with a TWDSW = 10 µs [4] [5]. The figures use a semilogarithmic scale for better readability. The figures clearly illustrate that the longer the line, the greater the benefits of the TW technology. The dependability curves in Fig. 24 and Fig. 25 are conservative estimates. In applications to short lines, the TW-based fault-locating methods do not abruptly lose dependability but gradually lose accuracy.
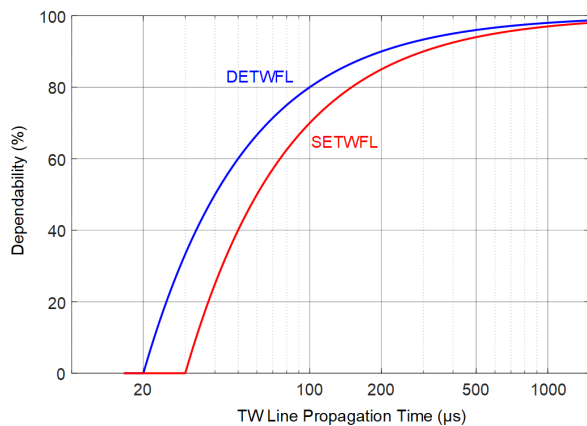

Fig. 24.   Dependability of the double-ended and single-ended methods as a function of the line propagation time.
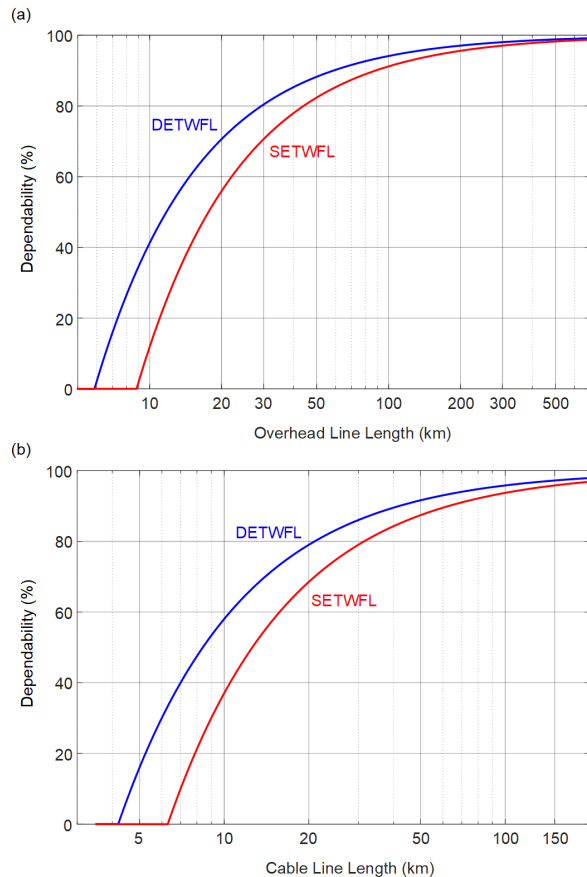

Fig. 25.   Dependability of the double-ended and single-ended methods as a function of the line length for an overhead line (a) and a cable line (b).

C.   Refining Dependability Contours in Special Cases

Let us consider a case when a certain fault location is near a discontinuity (such as a line tap) or when there is an external discontinuity that may reflect TWs and these TWs overlap with the key TWs in Fig. 20. Ideally, we would like the fault location to be away, by at least a TWDSW time interval in terms of the TW travel time, from 1) the line discontinuity and 2) an overlapping TW reflected from an external discontinuity. The per-unit distance, Δm, that a TW traveled during the TWDSW time is:

$$\Delta m = \frac{TWDSW}{TWLPT} = \delta \qquad (11)$$

Equation (11) means that a discontinuity will remove a portion of the dependability area in the shape of a triangle (the slope between Δm and δ is 1).

Fig. 26 shows an approximation of the dependability contour for the double-ended method when a line tap is located at 0.3 pu. The figure shows that dependability is impacted for fault locations near the tap. Again, the contour in Fig. 26 is a conservative estimation. Realistically, the tap will only skew the time stamp and result in degraded accuracy rather than a loss of function.
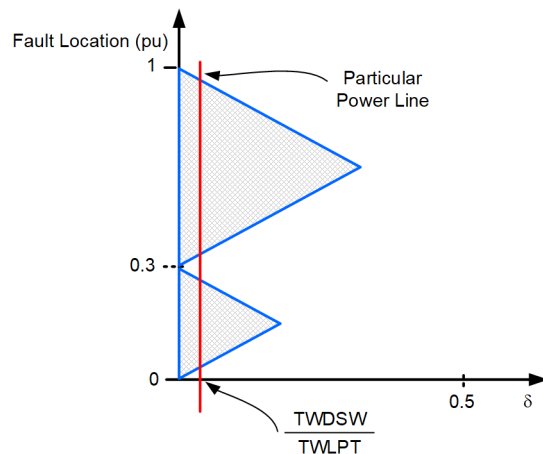

Fig. 26.   Dependability contour for the double-ended method when a line tap is present at 0.3 pu.

Fig. 27 shows an approximation of the dependability contour for the single-ended method when there is an external discontinuity located 0.8 pu from the local terminal. The figure shows that dependability of the single-ended method at the remote terminal is impacted for fault locations near the 0.8 pu location (see Fig. 16 for an explanation of the TW aliasing issue). Again, the contour in Fig. 27 is a conservative estimation. Realistically, the reflection from the external discontinuity is reduced by the termination effect and will only skew the time stamp and result in degraded accuracy rather than a loss of function. Also, if the fault-locating results from both line terminals are retrieved and used, the accuracy is improved.
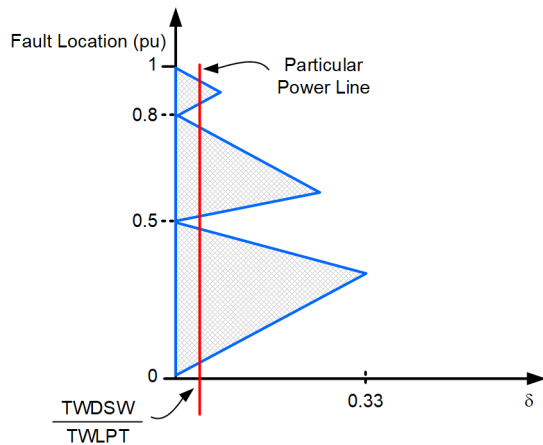
Fig. 27. Dependability contour for the single-ended method when an external discontinuity is present at 0.8 pu from the local terminal.

The method for evaluating the TW-based fault-locating dependability presented in this section allows us to draw the following conclusions:

- Discontinuities (line terminals, line taps, and external discontinuities if their reflected TWs propagate into the line) create "triangular holes" in the dependability contour.
- The areas of impaired dependability grow in terms of per-unit fault location as the line gets shorter.
- The presented dependability contours are conservative estimates; the field performance is typically better (reduced accuracy rather than loss of function).
- The "minimum line length" question for applicability of TW-based fault locating is not a yes-or-no question. Rather, for any given line length, one can expect a certain guaranteed (minimum) dependability of TW-based fault locating.
- The longer the line (the smaller the TWDSW/TWLPT ratio), the higher the dependability, and the lesser the impact of all discontinuities on the performance of TW-based fault locating.

D. Test Results for a Sample 30-Mile Line

Let us consider a sample 30 mi overhead line to illustrate the concepts of TW-based fault-locating dependability and accuracy. Devices [4] have been tested by using fault cases generated by using an electromagnetic transient program. This application involves a TWDSW = 10 μs (the DS filter window used in [4]) and a TWLPT = 164.3 μs (the TW propagation time of the 30 mi line). According to (4), $\delta = 0.0609$ and the theoretical conservative dependability is 88 percent for the double-ended method and 82 percent for the single-ended method.

Fig. 28 shows the theoretical dependability region and the accuracy of the double-ended method as tested. The figure shows that the method works for the entire line length, including fault locations as close to the terminals as 0.5 mi. The method is very accurate for faults within the dependability region (0.01 mi error) and accurate outside of the dependability region (0.05 mi error).
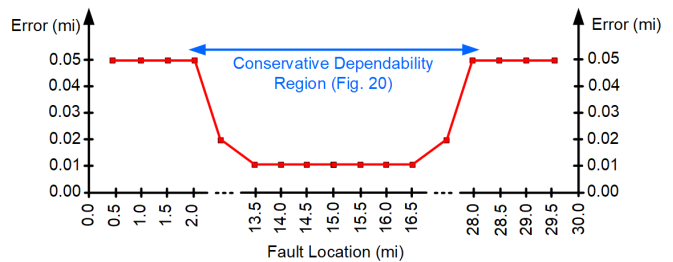

Fig. 28. Dependability interval and tested accuracy of the double-ended method applied to a 30 mi line.

Fig. 29 shows the theoretical dependability region and the accuracy of the single-ended method as tested. The figure shows that the method works for the entire line length except faults about 1 mi away from the line midpoint (see Fig. 14 and Fig. 22). The method is accurate for faults within the dependability regions (0.1 mi error) and slightly less accurate outside of the dependability regions (0.15 mi error). The single-ended method works for faults located at least 2 mi from the terminal (compare with Fig. 11 showing a field case of a fault located 2.1 mi from the terminal). Applying the single-ended method at the remote terminal covers the first 2 mi, and applying the single-ended method at the local terminal covers the last 2 mi. Download and use the fault-locating results from both terminals for dependable single-ended fault locating. The accuracy is slightly degraded for faults close to the opposite line terminal because of the skew in the time stamp of the TW reflection from the fault (TW_{R3} skews the time stamp of TW_{R2} in Fig. 9).
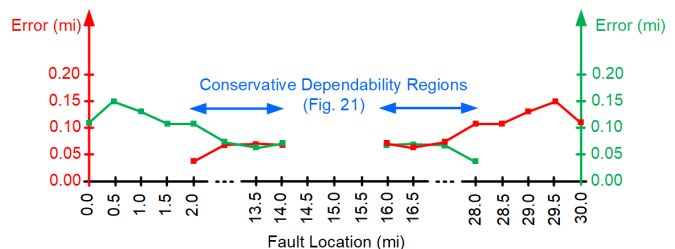

Fig. 29. Dependability interval and tested accuracy of the single-ended method applied to a 30 mi line.

If the single-ended TW-based method fails and the single-ended impedance-based method reports the fault near the line midpoint, assume the fault is indeed close to the line midpoint and verify the fault location by analyzing the transient record (see Section VII).

VII. FAULT ANALYSIS AND OFFLINE FAULT LOCATING

When performing fault analysis and offline fault locating by using ultra-high-resolution records, you have an option to adjust the DS filter window length. This includes shortening the window compared with the default length to allow detecting and time-stamping TWs that arrive in quick succession and also lengthening the window to allow better noise suppression and detecting and time-stamping of highly dispersed TWs. Some event analysis software [9] allows modifying the TWDSW parameter for the offline-calculated TWs. When using [9] to analyze transient records from [4] and [5], open the *.HDR IEEE COMTRADE file with a text editor (see Fig. 30) and edit

the TWDSW parameter before using [9] to open the record. Remember to restore the TWDSW parameter to its default value after analysis to avoid confusion when using the record again in the future.
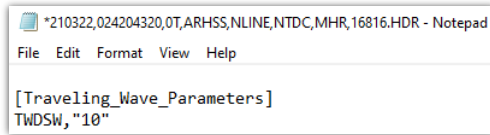

Fig. 30. Modifying the TWDSW parameter in a text editor before using [9] to analyze records from relays [4] and [5].

Follow these best practices with respect to the DS filter window length when analyzing fault records and performing offline fault locating:

- When using data from both line terminals, remember to use the same TWDSW parameter for both records. This ensures the same DS filter group delay. Otherwise, with different TWDSW parameters, the TW time stamps at the two line terminals must not be compared because of the unequal group delay. In advanced applications, you can correct for the unequal group delay as explained later in this section.

- If you encounter significant high-frequency ringing in the signals, consider adjusting the TWDSW to notch the ringing frequency out. Measure the period of the oscillatory signal component and select the TWDSW to be a multiple of the period. For example, to notch out a 3 μs ringing, select the TWDSW to be 6, 9, 12, or 15 μs.

- After you have obtained the first approximation of the time separation between two TWs, you can adjust the TWDSW to optimize noise rejection or sensitivity. The TWDSW parameter must not be more than half the TW separation time. For example, if the two TWs of interest arrive separated by 40 μs and you want to reduce the high-frequency noise, you can select a TWDSW as long as 20 μs (double the default of 10 μs). However, if the two TWs of interest arrive separated by 12 μs, you need to select a TWDSW as short as 6 μs to see these TWs individually.

- Start with the default TWDSW of 10 μs to gain a general understanding of the fault location, the TWs arriving at the terminal, and their polarities and arrival times. If needed, zoom in for selected TWs by reducing the TWDSW parameter or zoom out by increasing it. A shorter TWDSW reveals finer features but allows more noise. A longer TWDSW suppresses noise but potentially blends multiple TWs.

- You can obtain time stamps corrected for the DS filter group delay by subtracting the TWDSW value from the time of the DS filter output peak. For example, if the DS filter output peak time is 123.2 μs when using a TWDSW = 6 μs, you can record the corrected time stamp as 123.2 – 6 = 117.2 μs. The 117.2 μs time stamp is independent from the TWDSW parameter and can be compared with time stamps obtained with different TWDSW values. For example, you may

apply a TWDSW = 20 μs to the record at the other line terminal for better noise rejection and obtain the peak time from the DS filter output as 211.5 μs. After correcting for the DS filter group delay, you can compare the 211.5 – 20 = 191.5 μs time stamp with the 117.2 μs time stamp.

VIII. REVIEW OF TW-BASED FUNCTIONS IN RELATION TO LINE LENGTH AND FAULT LOCATION

This section reviews the impact of line length and fault location on typical TW-based functions, assuming the DS filter with the window half-length of 10 μs [4] [5].

A. Single-Ended TW-Based Fault Locating

The following observations apply to the single-ended method:

- The method is not effective on overhead lines shorter than about 10 km (6 mi) and cable lines shorter than about 6 km (4 mi). The method reaches 80 percent dependability for overhead lines longer than 50 km (30 mi) and cable lines longer than about 30 km (20 mi).

- The method may be less effective on very long lines and cable lines because of attenuation and dispersion. For example, if the fault is located 200 km (120 mi) from the terminal, the method responds to a TW that traveled 600 km (360 mi) after it was launched and before it arrived at the terminal as the first reflection from the fault.

- Offline applications of the method are possible on short lines by shortening the TWDSW when working with ultra-high-resolution transient records (see Section VII). Similarly, offline applications on long lines can give better results by lengthening the TWDSW.

- The method can perform poorly for fault locations that alias with locations of line terminals, line taps, and discontinuities outside of the protected line.

- The method has a dependability gap for faults in the middle of the line.

- The method can be challenged by reflections from network elements. Always inspect the impedance-based fault-locating results as a verification of the TW-based fault location and when selecting the TW-based fault location before dispatching the line crew.

- Typically, the local and remote line terminals have different operating conditions with respect to the single-ended method. Retrieve and inspect fault-locating results from both line terminals before dispatching the line crew.

B. Double-Ended TW-Based Fault Locating

The following observations apply to the double-ended method:

- The method may be less effective on overhead lines shorter than about 6 km (4 mi) and cable lines shorter than about 4 km (3 mi). The method reaches

80 percent dependability for overhead lines longer than 30 km (20 mi) and cable lines longer than about 20 km (12 mi). These threshold values are conservative estimates. The method works for shorter lines but with slightly degraded accuracy.

- The method can be applied to relatively long overhead lines and cable lines because it only uses the first TWs, and the first TWs travel less than the line length. For example, if the fault is located at 200 km (120 mi) on a 300 km (200 mi) line, the method works with TWs that travel 100 km (80 mi) and 200 km (120 mi) before they arrive at the line terminals.
- The method works well for faults close to terminals and taps, but it may have slightly degraded accuracy for such faults.
- Reflections from taps and network discontinuities do not affect this method because the first TWs are always launched by the fault and are never reflections. Subsequent TWs, if they arrive in quick succession, can skew the time stamps of the first TWs and erode some accuracy, but they cannot make the method fail.
- The method is reliable and accurate. If the method should provide inaccurate results, inspect the settings and verify that the time synchronization between the local and remote devices was accurate when the fault occurred.
- Offline applications of the method may be beneficial in special cases, especially on long cable lines when lengthening the TWDSW may allow detecting TWs with better sensitivity and time-stamping them with better accuracy.

C. TW-Based Line Monitoring

The TW-based line monitoring function leverages the double-ended method, and therefore it has the same line length limitations. However, unlike the fault-locating function, the line monitoring function may be configured to trigger on low-energy events with the intent to detect incipient faults and fault precursors. This high sensitivity can occasionally lead to false positives – external events detected and tabulated as internal events. The line monitoring function includes the logic to prevent false positives. If they occur, however, these false positives are typically tabulated at the line terminals (first and last bins [6]) because external events often launch TWs that pass through the monitored line. Occasionally, an external event can occur at a spot located at similar distances with respect to both terminals of the monitored line. If this event is a false positive, it is tabulated at the location with the same distance difference to the line terminals as the external event (see Fig. 31). If you suspect a false positive, search for spots located at the same distance difference with respect to the line terminals. For example, if an event is tabulated at 15 km on a 60 km line, and the event is a false positive, then the source of the event is located at the spot that is 30 km closer to the local terminal than to the remote terminal.
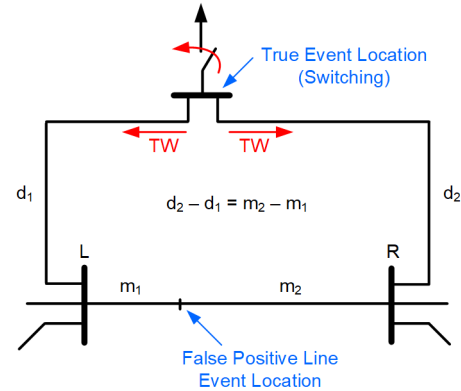

Fig. 31. Aliasing phenomenon explaining false positives in the line monitoring function.

D. TW87 Scheme

The TW87 scheme includes several security conditions. These conditions have yielded an excellent security record in the field for relays [4] and [5]. However, these security conditions may impact the TW87 scheme dependability, depending on the line length and fault location:

- The scheme must detect the first TWs at both line terminals, and these TWs must be relatively similar in shape to the ideal TW (step change). This requirement can make the scheme slightly less dependable for faults very close to the line terminals (see Fig. 4 and Fig. 5).
- The scheme verifies if the magnitudes of the first TWs at both line terminals as well as the sum of these first TWs are greater than certain minimum levels. This requirement can make the scheme less dependable in applications to long cable lines because of attenuation and dispersion, especially for faults away from the middle section of the line.
- The scheme assumes an external fault and verifies the presence of exit TWs to ensure security for external faults. If a discontinuity exists in the system and can reflect a TW in such a way that it arrives at the expected exit TW time for a specific internal fault (see Fig. 16), then the scheme may lose dependability for that internal fault.

In general, you can use the dependability of the double-ended method (see Fig. 23 and Fig. 25 as well as the dependability contours) to approximate the TW87 scheme dependability in relation to the line length and fault location. This approach results in a base dependability of 80 percent or higher. Other factors, such as excessive ringing in the secondary cables or faults that occurred when the instantaneous voltage was low, may reduce that initial dependability estimate.

E. TW32 Directional Element

In reference to Fig. 18, the TW32 element design in [4] and [5] requires the line to be long enough so that the TW reflected from the opposite terminal does not arrive within the TW32 data window, e.g., TW32WIN = 2 · 50 μs. Implementations [4] and [5] disable the TW32 logic for lines with a one-way TW propagation time (a relay setting) shorter than 50 μs. You

should refrain from using the TW32 element on tapped lines and hybrid overhead and cable lines if the discontinuity on the protected line is located at a distance shorter than 50 μs of travel time from the line terminal.

IX. CONCLUSIONS

This paper reviews the impact of line length and fault location on the dependability and accuracy of practical TW-based protection and fault-locating functions. The paper conclusions and observations apply directly to [4] and [5] and can be extended to [2] as well as any relay or fault locator that uses a window-based method for detecting and time-stamping TWs.

Line length is not the only factor that impacts the dependability and accuracy of TW-based functions. While it is true that very short lines do not allow effective applications, one should keep in mind that in most cases, the impact of a short line length or close-in fault location is limited accuracy and dependability rather than a total loss of function. Also, other factors beyond the line length and fault location play a role, such as line taps and other discontinuities internal or external to the protected line.

The double-ended method in [4] and [5] is highly dependable for overhead lines longer than about 30 km (20 mi) and it works well for overhead lines as short as 6 km (4 mi). The single-ended method requires longer line lengths and cannot be expected to perform for overhead lines shorter than about 10 km (6 mi); it reaches 80 percent dependability for overhead lines 50 km (30 mi) in length and longer. These numbers assume low-impedance line terminations, such as when each terminal connects two or more lines in addition to the line of interest.

The TW87 protection scheme and the line monitoring function incorporate the double-ended method in their logic. You can expect similar dependability and applicability limits for these functions as for the double-ended method.

The TW32 directional element in [4] and [5] cannot be applied on lines with a propagation time shorter than about 50 μs (about a 15 km (9 mi) overhead line) to ensure reflections from the opposite terminal do not arrive within the TW32 data window.

The paper proposes a methodology to calculate conservative dependability estimates for the single- and double-ended methods. Use these dependability contours to estimate dependability for a particular line given the DS filter window length.

Faults located very close to line terminals and other discontinuities, such as taps or overhead-to-cable transition points, challenge the single-ended method but not the double-ended method. At worst, the double-ended method may display a slightly reduced accuracy for such faults.

Cable lines attenuate and disperse TWs much more than overhead lines. TW-based functions are challenged when used for cable lines that are too long to allow TWs to arrive at the line terminals with magnitudes great enough and wavefronts sharp enough for reliable detection and time-stamping. The cable line length limitation depends on the voltage level. The greater the voltage, the longer the cable.

The operating conditions may be different for the double-ended method and the local and remote single-ended methods depending on the fault location with respect to the line terminals and discontinuities. For example, if the fault is located close to the local terminal but the cable line attenuation prevents the double-ended method from providing the result, the local single-ended method may work satisfactorily. Or, when a very close-in fault prevents the local single-ended method from providing the result, the remote single-ended method may work satisfactorily. By retrieving and using all three results (double-ended, local single-ended, and remote single-ended), you can overcome many of the line length constraints.

Devices [4] and [5] work with DS filter lengths that have been selected for secure protection and accurate fault locating. When performing fault analysis and offline fault locating by using relay records, you can adjust the DS filter window length and balance the need for noise rejection and time-stamping resolution. Offline fault locating can be performed in multiple steps by adjusting the DS filter window length based on information gained in previous steps. This allows you to resolve challenging and unusual cases that include tapped lines, lines with unusual terminations, and hybrid lines.

X. REFERENCES

[1] E. O. Schweitzer, III, A. Guzmán, M. V. Mynam, V. Skendzic, B. Kasztenny, and S. Marx, "Locating Faults by the Traveling Waves They Launch," proceedings of the 40th Annual Western Protective Relay Conference, Spokane, WA, October 2013.

[2] SEL-411L Advanced Line Differential Protection, Automation, and Control System Instruction Manual. Available: https://selinc.com.

[3] E. O. Schweitzer, III, B. Kasztenny, A. Guzmán, V. Skendzic, and M. V. Mynam, "Speed of Line Protection – Can We Break Free of Phasor Limitations?" proceedings of the 41st Annual Western Protective Relay Conference, Spokane, WA, October 2014.

[4] SEL-T400L Time-Domain Line Protection Instruction Manual. Available: https://selinc.com.

[5] SEL-T401L Ultra-High-Speed Line Relay Instruction Manual. Available: https://selinc.com.

[6] B. Kasztenny, M. V. Mynam, T. Joshi, and D. Holmbo, "Preventing Line Faults With Continuous Monitoring Based on Current Traveling Waves," proceedings of the 15th International Conference on Developments in Power System Protection, Liverpool, UK, March 2020.

[7] B. Kasztenny, A. Guzmán, N. Fischer, M. V. Mynam, and D. Taylor, "Practical Setting Considerations for Protective Relays That Use Incremental Quantities and Traveling Waves," proceedings of the 43rd Annual Western Protective Relay Conference, Spokane, WA, October 2016.

[8] A. Sivesind, F. J. Sanchez, S. Cooper, F. Elhaj, "Traveling Wave Relay Application, Commissioning, and Initial Experience," presented at the 72nd Annual Conference for Protective Relay Engineers, College Station, TX, March 2019. Available: https://prorelay.tamu.edu/archive/.

[9] SYNCHROWAVE Event Software Instruction Manual. Available: https://selinc.com.

XI. BIOGRAPHIES

Bogdan Kasztenny has over 30 years of experience in power system protection and control. In his decade-long academic career (1989–99), Dr. Kasztenny taught power system and digital signal processing courses at several universities and conducted applied research for several relay manufacturers. In 1999, Bogdan left academia for relay manufacturers where he has since designed, applied, and supported protection, control, and fault-locating products with their global installed base counted in thousands of installations. Bogdan is an IEEE Fellow, a Senior Fulbright Fellow, a Distinguished CIGRE

Member, and a registered professional engineer in the province of Ontario. Bogdan has served as a Canadian representative of the CIGRE Study Committee B5 (2013–2020) and on the Western Protective Relay Conference Program Committee (2011–2020). In 2019, Bogdan received the IEEE Canada P. D. Ziogas Electric Power Award. Bogdan earned both the Ph.D. (1992) and D.Sc. (Dr. habil., 2019) degrees, has authored over 220 technical papers, and holds over 50 U.S. patents.

Mangapathirao (Venkat) Mynam received his MSEE from the University of Idaho in 2003 and his BE in electrical and electronics engineering from Andhra University College of Engineering, India, in 2000. He joined Schweitzer Engineering Laboratories, Inc. (SEL) in 2003 as an associate protection engineer in the engineering services division. He is presently working as an engineering director in SEL research and development. He was selected to participate in the U. S. National Academy of Engineering (NAE) 15th Annual U. S. Frontiers of Engineering Symposium. He is a senior member of IEEE and holds patents in the areas of power system protection, control, and fault location.